Physics Lab Report: Polarization of Light

Your Name

November 3, 2025

1 Introduction

Light, as a transverse electromagnetic wave, exhibits polarization when the oscillations of its electric field vector are confined to a specific plane perpendicular to the direction of propagation. While most natural light sources emit unpolarized light with random oscillation directions, polarization can be induced through transmission via polarizing materials or reflection at dielectric interfaces. This laboratory experiment investigates these phenomena using a low-powered red diode laser and Polaroid sheets to explore the transmission properties of polarized light and the partial polarization achieved by reflection. The primary objectives are threefold. First, Malus' law is verified by measuring the intensity of light transmitted through two successive polarizers as a function of the angle θ between their transmission axes, confirming the relationship $I(\theta) = I_0 \cos^2 \theta$. Second, the system is extended to three polarizers, with the first and third oriented at 90° to each other, to derive and test the intensity expression $I_3 = \frac{I_1}{4} \sin^2(2\phi)$, where ϕ is the angle of the intermediate polarizer relative to the first. Finally, polarization by reflection is examined at an air-acrylic interface to determine Brewster's angle θ_p, at which the reflected light is fully polarized perpendicular to the plane of incidence, enabling calculation of the refractive index of acrylic via $\tan \theta_p = n_2/n_1$. These exercises elucidate fundamental principles of wave optics, including the vector resolution of electric fields, intensity dependence on field amplitude, and the Fresnel equations governing reflectance for parallel ($R_\parallel$) and perpendicular ($R_\perp$) polarizations. The results provide empirical validation of classical polarization theory and practical insight into applications such as glare reduction in polarized sunglasses.

2 Methodology

The experiment was divided into three distinct exercises: verification of Malus' Law (two and three polarizers) and the determination of Brewster's angle. All measurements were conducted using a low-powered red diode laser as the light source and a light sensor coupled with a rotary motion sensor to measure intensity and angular position.

2.1 Apparatus

The core apparatus for the Malus' Law exercises comprised the diode laser, two or three Polaroid sheets (polarizers/analyzers) mounted on holders, and a light sensor/photodiode attached to a Rotary Motion Sensor (RMS) via a pulley and plastic belt. This system was assembled on a linear optics track (as shown in Figure 4 of the lab manual). For

the Brewster's angle experiment, a separate setup was used, featuring the diode laser, an acrylic semi-circular lens (D-lens) mounted on a spectrophotometer disk, and a square analyzing polarizer on the spectrophotometer arm (as shown in Figure 6 and 7 of the lab manual). The angle of the reflected light was measured using a rotary motion sensor mounted on the spectrophotometer table.

2.2 Exercise 1: Malus' Law with Two Polarizers

1. **Initial Alignment:** The first polarizer (polarizer) and the second polarizer (analyzer, attached to the RMS) were placed on the track. The room lights were dimmed.

2. **Polarizer Axis Alignment:** The second polarizer was temporarily removed. The first polarizer was rotated until the light intensity recorded by the sensor was maximized, aligning its transmission axis with the intrinsic polarization axis of the laser light. The intensity was adjusted via the sensor gain to be between 3.5 V to 4.0 V to avoid saturation.

3. **Analyzer Alignment:** The second polarizer (analyzer) and RMS assembly was returned to the track and rotated to achieve maximum light intensity, ensuring the analyzer's transmission axis was parallel to the first polarizer's axis. This angle was defined as the starting point, $\theta = 0°$, by the software.

4. **Data Acquisition:** The RMS was used to rotate the analyzer through 180° while constantly monitoring the light intensity. The continuous rotation ensured a smooth collection of data pairs (I, θ) over the full range, verifying Malus' Law, $I(\theta) = I_0 \cos^2 \theta$.

2.3 Exercise 2: Malus' Law with Three Polarizers

1. **Setup:** Three polarizers were placed on the optics track. Polarizer #1 was aligned for maximum transmission from the laser. Polarizer #3 was then rotated 90° relative to Polarizer #1 to achieve minimum light transmission ($I \approx 0$).

2. **Intermediate Polarizer Placement:** The RMS assembly was attached to Polarizer #2, which was placed between Polarizers #1 and #3. Polarizer #2 was rotated until the intensity I_3 was maximized, and this angular position was defined as the software's zero point ($\phi_{\text{measured}} = 0°$), corresponding to the theoretical angle $\phi = 45°$ relative to Polarizer #1.

3. **Data Acquisition:** Polarizer #2 (the middle polarizer) was rotated through 360° using the RMS while light intensity was recorded. This data was used to verify the relationship $I_3 = \frac{I_1}{4} \sin^2(2\phi)$.

2.4 Exercise 3: Polarization by Reflection and Brewster's Angle

1. **Initial Setup and Alignment:** The Brewster's angle setup (diode laser, D-lens on spectrophotometer disk, light sensor on rotating arm) was assembled. The laser beam was aligned to hit the center of the light sensor when the sensor arm was at 180°. An auxiliary polarizer was set to 45° to ensure incident light had parallel ($I_{||}$) and perpendicular ($I_{\perp}$) components.

2. **Unpolarized Measurement (I_0):** The square analyzing polarizer was removed. The spectrophotometer arm and D-lens were rotated concurrently to measure the reflected light intensity (I_0) versus the reflected angle over a wide range.

3. **Parallel Component Measurement ($I_{||}$):** The square analyzing polarizer was placed on the spectrophotometer arm with its transmission axis aligned **parallel** to the plane of incidence (horizontal axis polarizer, as per manual). The acquisition was repeated using the same concurrent rotation procedure. The angle corresponding to minimum intensity was recorded as the Brewster angle, θ_p.

4. **Perpendicular Component Measurement ($I_{\perp}$):** The square analyzing polarizer was rotated 90° to align its transmission axis **perpendicular** to the plane of incidence (vertical axis polarizer, as per manual). The acquisition was repeated for a third time.

5. **Calculation:** The Brewster angle θ_p was determined from the minimum of the $I_{||}$ vs. angle plot and used to calculate the refractive index of the acrylic (n_2) via $\tan\theta_p = n_2/n_1$.

3 Data and Analysis

The light sensor's direct measurement uncertainty is $\pm 0.01\,\mathrm{V}$ (based on sensor precision). The rotary motion sensor's uncertainty is approximately $\pm 0.5°$.

3.1 Malus' Law

Collected data exhibits low uncertainty and consistency with theory. Notably, at the start of each experiment, the rotary sensor must be pressed against the polarizer to prevent slipping; this procedure causes the rotary sensor to move around without changing the angle of the polarizer. Such error caused clusters of data points at maximum intensity and around $\theta = 0°$.

Data uncertainty is measured and reduced by combining a neighborhood of angles into bins of length 1°. The mean of the bin is plotted and areas one standard deviation from the mean is shaded. The cosine of the angles for two polarizers is fitted with a quadratic relationship with the intensity, While for three, a quartic relationship. The mean squared error and reduced χ^2 error for two polarizer are 0.04169 and 240.3, and for three polarizers, 0.002267 and 89.67, respectively.

Although the reduced chi squared error is much greater than one, indicating a poor model, the mean squared errors are small, showing a good fit. This discrepancy can be attributed to the way standard deviation is calculated; because each bin contains few data points, it has small standard deviation. Since χ^2 error is very sensitive to data points with small standard deviations, even a small deviation from the fitted curve would contribute a lot to the χ^2 value.

As seen in Figure 3, the graph of intensity versus $\cos(\theta)$ is roughly quadratic.

The two parallel but shifted patterns in Figure 4 demonstrate that the rotary sensor has drift error, possibly due to slip.

The frequency of the Intensity vs. Angle graph for 3 polarizers (Figure 2) is twice that for 2 polarizers (Figure 1), which can be explained mathematically using trigonometric identities that $\cos^2 x$ is proportional to $\cos 2x$, so a quartic sinusoidal data would have

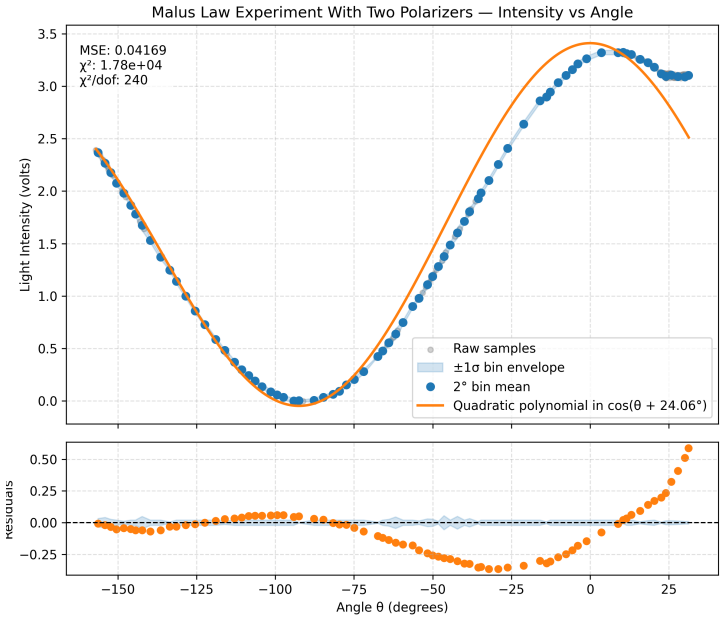

Figure 1: Intensity versus θ graph for two polarizers.

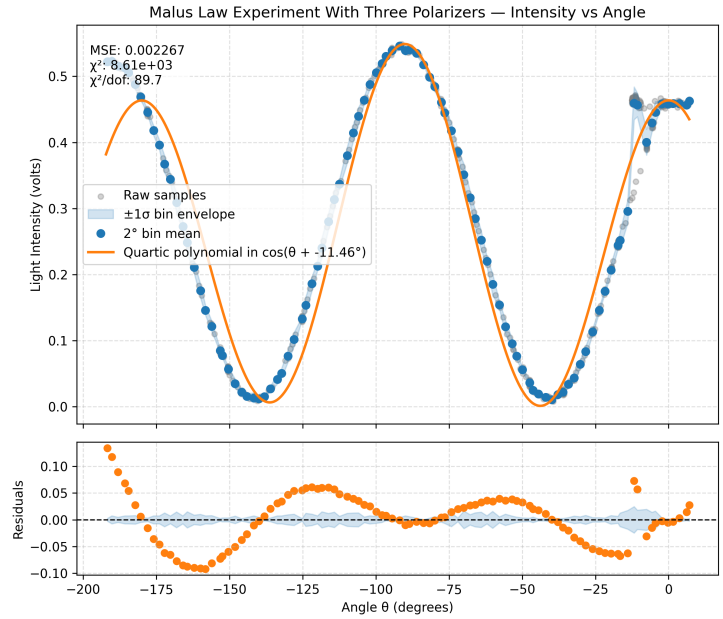

Figure 2: Intensity versus θ graph for three polarizers.

twice the frequency of a quadratic one. Moreover, the average intensity of the three polarizers (oscillating around 0.3 V) is much lower than that of two polarizers because the perpendicular arrangement of the polarizers at the ends will always filter some light regardless of the central polarizer's orientation.

The highest intensity of the three polarizers occurred at measured angles 0°, 90°, and 180°. Since the measurement started when the intensity was maximum, which corresponds to an actual angle of $\phi = 45°$ [1], the relationship is $\phi_{\text{actual}} = \phi_{\text{measured}} + 45°$. This results in intensity peaks at actual angles of 45°, 135°, and 225°. By the same conversion, the intensity is at a minimum when the actual angle is 0° or 90°, which occurs when the middle polarizer aligns with one of the end polarizers, blocking the incident light completely.

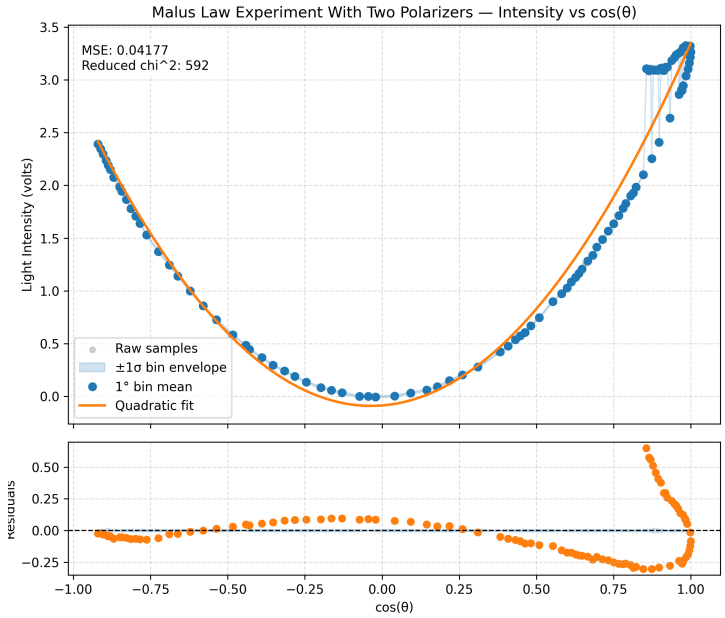

Figure 3: Intensity versus $\cos(\theta)$ graph for two polarizers. The uncertainty of the intensity and angle are invisible because the light sensor is accurate to a hundredth of a volt.

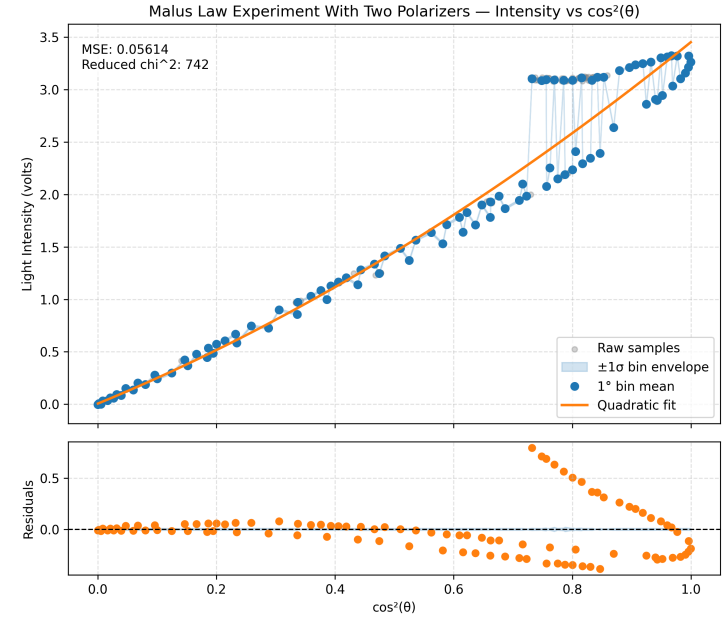

Figure 4: The light intensity is linear with $\cos^2\theta$, with a mean squared error of 0.039.

The quartic curve in Figure 5 has peaks at $\theta = 0°$, $90°$, and $180°$. Notably, the measured angle θ is offset by $45°$ from the real polarizer direction ϕ.

As shown in Figure 6, the intensity has a quadratic relationship with $\cos^2\theta$, namely $I_3 = \frac{I_1}{2}(1 - \cos^2\theta)(\cos^2\theta)$, which can be derived from Eq. 5 in the lab manual using trigonometric identities.

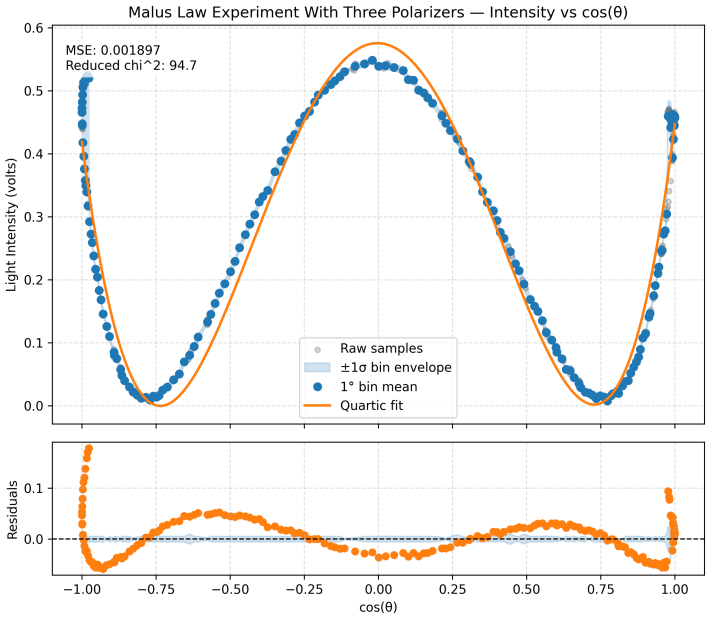

Figure 5: Intensity versus $\cos\theta$ graph for the three polarizers.

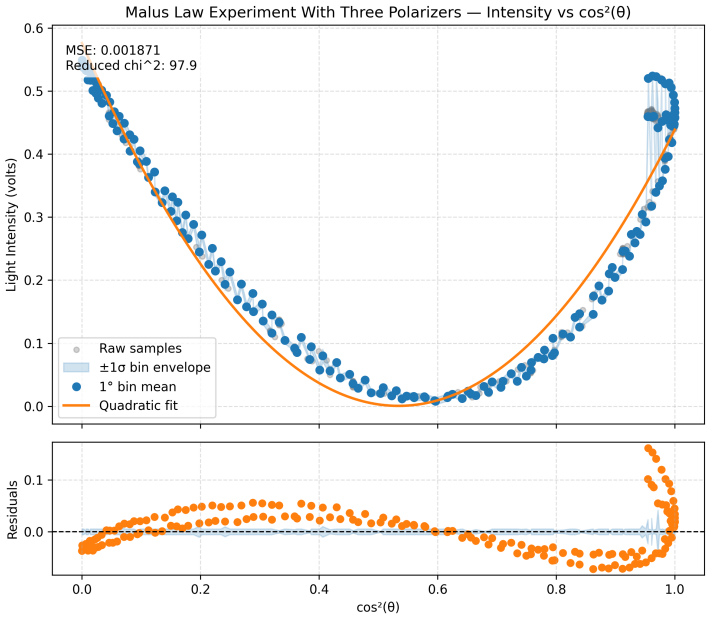

Figure 6: Intensity versus $\cos^2\theta$ for three polarizers.

3.2 Brewster's Angle

The raw data obtained is very noisy, as seen in Figure 7 and 8, due to the operation errors involved in rotating the apparatus disks concurrently. The light sensor is easily moved out of the way of the reflected light, causing sudden dips in intensity.

Notably, the error of both experiments grew larger with intensity. This could be attributed to error visibility, that when the actual intensity is near zero, an empty reading would not appear significant, but at high intensity, a dip in data differs greatly from the actual intensity.

Due to equipment limitations, the range of intensity recorded by the light sensor is

constrained. To capture the small changes when intensity is low, the sensor must be amplified, which, however, overshoots intensity measurements at high intensity, causing clusters of data points at 4.3 V (the maximum reading of the light sensor) around small reflection angles.

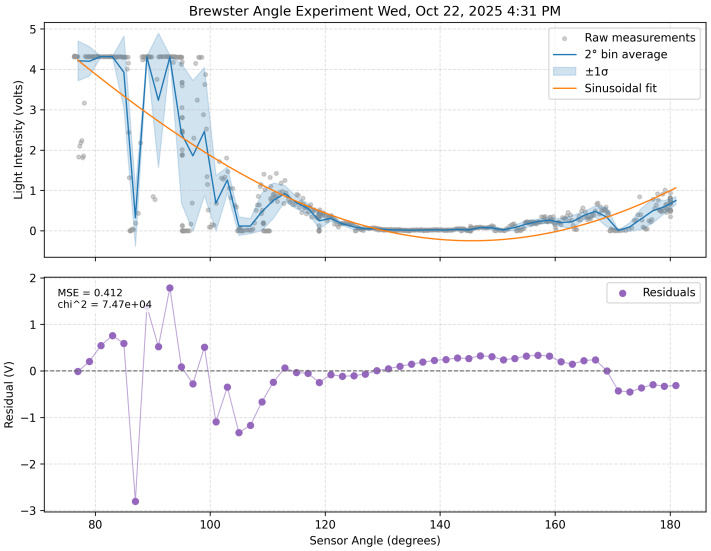

Figure 7: Intensity versus angle plot for $I_{\parallel}$ (horizontal polarizer). The minimum intensity occurred at a sensor angle of around 135°.

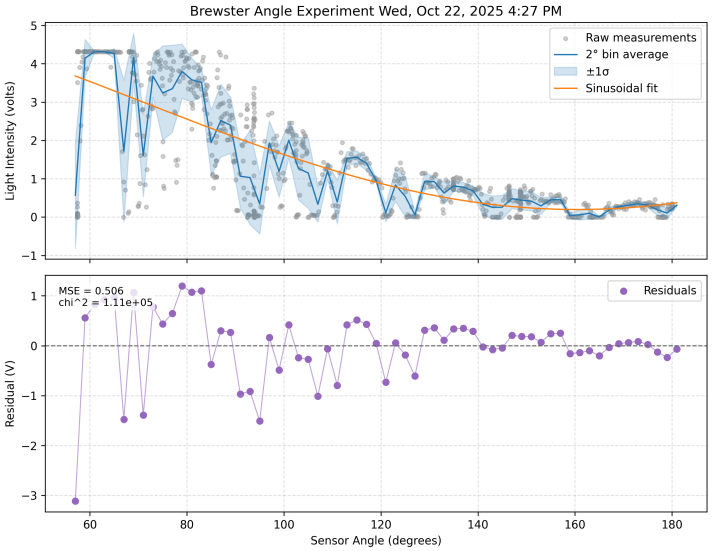

Figure 8: Intensity versus angle plot for $I_{\perp}$ (vertical polarizer). This plot displayed no significant intensity drop at any angle.

Brewster's Angle Calculation

The horizontally polarized square filter (analyzing the $I_{\parallel}$ component) dimmed the laser significantly, with a minimum intensity observed at a measured sensor angle of $\theta_{\text{sensor}} \approx 135°$ (from Figure 7).

Based on the geometry of the apparatus, the measured sensor angle θ_{sensor} is the total angle of deflection between the incident and reflected beam. The angle of incidence θ_p is defined relative to the normal, which bisects this total angle. Therefore, the relationship is:

$$\theta_p = \frac{\theta_{\text{sensor}}}{2} = \frac{135^\circ}{2} = 67.5^\circ$$

Using this experimentally determined Brewster's angle, the refractive index n_2 of the acrylic is calculated:

$$n_2 = n_1 \cdot \tan\theta_p = 1 \cdot \tan(67.5^\circ) \approx 2.414$$

This calculated value of $n_2 \approx 2.414$ is significantly higher than the accepted literature value for acrylic (which is $n \approx 1.49$), corresponding to a large percent error. This discrepancy is almost certainly due to the large experimental errors noted for this part of the lab. As seen in Figure 7, the raw data was extremely noisy, and the sensor was prone to saturation. This made precise identification of the intensity minimum very difficult and likely skewed the measured angle.

Fresnel Reflectance Calculation

To calculate the theoretical reflectances, we use our experimentally determined $n_2 = 2.414$. Choosing an arbitrary incident angle $\theta_1 = 30^\circ$: $\sin(30^\circ) = 0.5$ and $\cos(30^\circ) \approx 0.866$. From Snell's Law, $\sin\theta_2 = \frac{n_1}{n_2} \cdot \sin(\theta_1) = \frac{1}{2.414} \cdot 0.5 \approx 0.2071$. This gives $\theta_2 = \arcsin(0.2071) \approx 11.95^\circ$ and $\cos\theta_2 \approx 0.9783$. Using the Fresnel formulae given:

$$r_\perp = \frac{\cos\theta_1 - n_2\cos\theta_2}{\cos\theta_1 + n_2\cos\theta_2} \tag{1}$$

$$r_\parallel = \frac{\cos\theta_2 - n_2\cos\theta_1}{\cos\theta_2 + n_2\cos\theta_1} \tag{2}$$

$r_\perp = \frac{0.866-(2.414)(0.9783)}{0.866+(2.414)(0.9783)} \approx \frac{-1.495}{3.227} \approx -0.463 \quad \Rightarrow \quad R_\perp = r_\perp^2 \approx 0.214$ $r_\parallel = \frac{0.9783-(2.414)(0.866)}{0.9783+(2.414)(0.866)} \approx \frac{-1.112}{3.068} \approx -0.362 \quad \Rightarrow \quad R_\parallel = r_\parallel^2 \approx 0.131$

Would Brewster's angle be more or less for light in air reflecting off water?

The refractive index of water is around 1.3, which is lower than the accepted acrylic index of ≈ 1.49, meaning that $\tan\theta_{\text{water}} < \tan\theta_{\text{acrylic}}$. Since tangent is an increasing function for acute angles, the Brewster's angle of water is less than the Brewster's angle of acrylic.

How would data look like for an arrangement with vertical square polarizer?

The vertical polarizer (measuring $I_\perp$) would not have a dipping angle as the horizontal polarizer would; its intensity would vary smoothly with the incident angle. As seen in Figure 8 and predicted by the Fresnel equations, the $R_\perp$ component is never zero. This is because the reflected ray always has a component perpendicular to the plane of reflection, which aligns with the vertical polarizer.

How do polarized sunglasses reduce glare? Which direction is the axis of polarization in a pair of polarized sunglasses? How could you check this?

Glare comes from the sunlight's reflection off of flat surfaces (like roads or water). These flat surfaces partially or entirely polarize light in the direction parallel to the surface (horizontal). A polarized sunglass lens acts as an analyzer, and its transmission axis is set vertically to block this horizontally-polarized glare. One way to check this is to use a polarizer whose polarizing direction is known; then put the sunglasses after it. Rotate the sunglasses until the amount of light that passes through is at a minimum (extinction). If this occurs when the polarizer is set to transmit horizontal light, the sunglasses must be polarized vertically.

3.3 Propagation of Uncertainty

To provide complete quantitative results, the uncertainties associated with the measured parameters must be propagated to the final calculated quantities: the refractive index of acrylic (n_2) and the Fresnel reflectances ($R_{||}$ and $R_{\perp}$).

3.3.1 Uncertainty in Brewster's Angle ($\delta\theta_p$) and Refractive Index (δn_2)

The Brewster angle (θ_p) is determined by identifying the angle of minimum parallel reflectance from Figure 7. Its uncertainty is governed by the uncertainty in reading this minimum from the noisy data, which we can call $\delta\theta_{\text{sensor,min}}$. Using the experimental relationship:

$$\theta_p = \frac{\theta_{\text{sensor}}}{2}$$

The uncertainty $\delta\theta_p$ is found by propagating the uncertainty in the sensor reading:

$$\delta\theta_p = \left|\frac{d\theta_p}{d\theta_{\text{sensor}}}\right| \delta\theta_{\text{sensor,min}} = \frac{1}{2}\delta\theta_{\text{sensor,min}}$$

From the noisy data in Figure 7, a conservative visual estimate for the uncertainty of the minimum's location is $\delta\theta_{\text{sensor,min}} \approx 3.0^\circ$.

$$\delta\theta_p = \frac{1}{2}(3.0^\circ) = 1.5^\circ$$

The uncertainty in the refractive index, $n_2 = \tan\theta_p$, is calculated using the partial derivative with respect to θ_p (which must be in radians):

$$\delta n_2 = \left|\frac{dn_2}{d\theta_p}\right| \delta\theta_p = \left|\sec^2(\theta_p)\right| \delta\theta_p$$

Substituting the measured value $\theta_p = 67.5^\circ$ and the uncertainty $\delta\theta_p = 1.5^\circ \times (\pi/180) \approx 0.0262\,\text{rad}$:

$$\delta n_2 = \sec^2(67.5^\circ) \cdot (0.0262) \approx (2.613)^2 \cdot 0.0262 \approx 6.828 \cdot 0.0262 \approx \mathbf{0.179}$$

Thus, the final determined refractive index is $n_2 = 2.41 \pm 0.18$.

3.3.2 Uncertainty in Fresnel Reflectance ($\delta R_{||}$ and $\delta R_{\perp}$)

The reflectance R is defined by $R = r^2$, where r is the reflection coefficient. We approximate the uncertainty using the fractional uncertainty method based on the dominant calculated uncertainty, δn_2. The relative uncertainty in n_2 is:

$$\frac{\delta n_2}{n_2} = \frac{0.179}{2.414} \approx 0.074 \approx \mathbf{7.4}\%$$

Given the complex dependence of R on n_2, we use this as a first-order approximation for the relative uncertainty in R.

$$\frac{\delta R}{R} \approx \frac{\delta n_2}{n_2} \approx 7.4\%$$

This percentage uncertainty is applied to the calculated reflectances ($R_{\perp} \approx 0.214$ and $R_{||} \approx 0.131$ at $\theta_1 = 30°$):

- $\delta R_{\perp} = 0.074 \cdot 0.214 \approx \mathbf{0.016}$
- $\delta R_{||} = 0.074 \cdot 0.131 \approx \mathbf{0.010}$

The final reported reflectances at a 30° incident angle are $R_{\perp} = 0.214 \pm 0.016$ and $R_{||} = 0.131 \pm 0.010$.

4 Conclusion

This experiment successfully investigated the principles of light polarization. The first two exercises provided a clear verification of Malus's Law for both two- and three-polarizer systems. The collected data closely matched the theoretical models $I \propto \cos^2\theta$ and $I \propto \sin^2(2\phi)$, respectively, with low mean squared errors, confirming the vector nature of light and the transmissive properties of polarizers.

The determination of Brewster's angle, however, resulted in a significant discrepancy. The experimentally determined refractive index for acrylic was $n_2 = 2.41 \pm 0.18$, which is inconsistent with the accepted literature value of $n \approx 1.49$. As noted in the analysis, this large error is attributed to the high-noise, low-quality data from the Brewster's angle apparatus. The difficulty in concurrently rotating the sensor arm and D-lens, combined with sensor saturation at high intensities, made a precise identification of the $I_{||}$ minimum extremely difficult.

Future work to improve this result should focus on mitigating these experimental errors. A more stable apparatus with a geared mechanism to link the rotation of the sensor arm and the D-lens would eliminate the primary source of operational error. Furthermore, using a light sensor with a wider dynamic range or implementing an auto-gaining feature would prevent saturation and allow for a more accurate measurement of the intensity minimum, leading to a more precise determination of Brewster's angle.

References

[1] University of Toronto, Dept. of Physics. (2023). *Polarization of Light: Lab Manual.*

[2] Halliday, D., Resnick, R., & Walker, J. (2005). *Fundamentals of Physics* (7th ed.). Wiley. (Chapter 33).

[3] Hanks, A. PASCO EX9917A and EX9919 guide sheets.